NEOPLASIA
www.neoplasia.com

Volume 18 Number 7 July 2016 pp. 436–446 436

Elevated VEGF-D Modulates Tumor Inflammation and Reduces the Growth of Carcinogen-Induced Skin Tumors[1]

Hanne-Kaisa Honkanen*, Valerio Izzi*, Tiina Petäistö*, Tanja Holopainen†, Vanessa Harjunen*,†, Taina Pihlajaniemi*, Kari Alitalo† and Ritva Heljasvaara*

*Oulu Center for Cell-Matrix Research, Biocenter Oulu and Faculty of Biochemistry and Molecular Medicine, FIN-90014, University of Oulu, Oulu, Finland; †Wihuri Research Institute and Translational Cancer Biology Program, Biomedicum Helsinki, University of Helsinki, FIN-00290, Helsinki, Finland

Abstract

Vascular endothelial growth factor D (VEGF-D) promotes the lymph node metastasis of cancer by inducing the growth of lymphatic vasculature, but its specific roles in tumorigenesis have not been elucidated. We monitored the effects of VEGF-D in cutaneous squamous cell carcinoma (cSCC) by subjecting transgenic mice overexpressing VEGF-D in the skin (K14-mVEGF-D) and VEGF-D knockout mice to a chemical skin carcinogenesis protocol involving 7,12-dimethylbenz[a]anthracene and 12-O-tetradecanoylphorbol-13-acetate treatments. In K14-mVEGF-D mice, tumor lymphangiogenesis was significantly increased and the frequency of lymph node metastasis was elevated in comparison with controls. Most notably, the papillomas regressed more often in K14-mVEGF-D mice than in littermate controls, resulting in a delay in tumor incidence and a remarkable reduction in the total tumor number. Skin tumor growth and metastasis were not obviously affected in the absence of VEGF-D; however, the knockout mice showed a trend for reduced lymphangiogenesis in skin tumors and in the untreated skin. Interestingly, K14-mVEGF-D mice showed an altered immune response in skin tumors. This consisted of the reduced accumulation of macrophages, mast cells, and $CD4^+$ T-cells and an increase of cytotoxic $CD8^+$ T-cells. Cytokine profiling by flow cytometry and quantitative real time PCR revealed that elevated VEGF-D expression results in an attenuated Th2 response and promotes M1/Th1 and Th17 polarization in the early stage of skin carcinogenesis, leading to an anti-tumoral immune environment and the regression of primary tumors. Our data suggest that VEGF-D may be beneficial in early-stage tumors since it suppresses the pro-tumorigenic inflammation, while at later stages VEGF-D-induced tumor lymphatics provide a route for metastasis.

Neoplasia (2016) 18, 436–446

Introduction

Non-melanoma skin cancer (NMSC) is the most frequent human cancer worldwide and its incidence is increasing among Caucasian people due to population aging. Approximately 20% of NMSCs are cutaneous squamous cell carcinomas (cSCC) and it is the second most common subtype after basal cell carcinoma. cSCC is mainly caused by repeated exposure to solar ultraviolet radiation throughout life, but, for example, chronic ulcers, ionizing radiation, chemicals, papillomavirus infection, and immunosuppressive medication are also risk factors. Approximately 20% of all the skin cancer related deaths are caused by metastatic cSCC. The average rate of the nodal metastasis of cSCC is around 5%, and the five-year survival rate of metastatic cSCC is less than 35% [1–4]. Metastatic cSCC most often spreads via tumor-associated lymphatic vessels to sentinel and distant lymph

Abbreviations: cSCC, cutaneous squamous cell carcinoma; DMBA, 7,12-dimethylbenz[a]anthracene; IFN, interferon; IL, interleukin; K14, keratin 14; KO, knockout; LN, lymph node; NMSC, non-melanoma skin cancer; TG, transgenic; TGF, transforming growth factor; TNF, tumor necrosis factor; TPA, 12-O-tetradecanoylphorbol-13-acetate; VEGF, vascular endothelial growth factor; VEGFR, vascular endothelial growth factor receptor; WT, wild type

Address all correspondence to: Ritva Heljasvaara, Faculty of Biochemistry and Molecular Medicine, University of Oulu, PO Box 5400, FIN-90014, Oulu, Finland.
E-mail: ritva.heljasvaara@oulu.fi

[1] This study was supported by the Research Council for Health of the Academy of Finland (Grants 138866 and 128259, and Centre of Excellence 2012–2017 Grant 251314), and by the Sigrid Jusélius Foundation. H-K.H. was supported by personal grants from the Emil Aaltonen Foundation and the Cancer Society of Northern Finland.
Received 4 January 2016; Revised 6 May 2016; Accepted 13 May 2016

1476-5586
http://dx.doi.org/10.1016/j.neo.2016.05.002

nodes (LNs), and sometimes also to distant organs, preferentially to other sites of the skin as well as to the lungs, liver, brain, and bone [5].

Increasing experimental and clinical evidence suggests that the growth of tumor-associated lymphatic vessels, in other words, tumor lymphangiogenesis, is actively induced in many tumor types [6], including cSCC [7], and that it promotes early LN metastasis. The extent of tumor lymphangiogenesis has also been suggested to serve as an independent predictor of LN metastasis and patient survival [8,9].

Vascular endothelial growth factors (VEGFs) C and D (the c-fos-induced growth factor [FIGF]) are key stimulators of lymphangiogenesis. They activate the VEGF receptor 3 (VEGFR-3) that is constitutively expressed in lymphatic endothelium [10,11]. At least in part, the signals from VEGFR-3 are transduced via the protein kinase C-dependent activation of the MEK/ERK1/2 mitogen-activated protein kinase signaling cascade and induction of Akt1 phosphorylation [12]. VEGFR-3 is expressed also in angiogenic blood vessel endothelia in tumors and thus signaling through VEGFR-3 can activate tumor angiogenesis [13]. While VEGF-C is essential for the formation of lymphatic vasculature during embryonic development [14], VEGF-D is not [15,16]. Nevertheless, a detailed analysis of dermal lymphatic network in the *Vegfd*$^{-/-}$ mice showed that this factor is needed for the maintenance of caliber and functional capacity of initial lymphatics [17]. In humans, both ligands can also bind to VEGFR-2 on blood vascular endothelial cells to activate angiogenesis and to support primary tumor growth and metastasis [18]. In contrast to human VEGF-D, mouse VEGF-D only binds to VEGFR-3 [19].

High VEGF-C or VEGF-D expression has been shown to boost VEGFR-3-mediated signaling to promote tumor lymphangiogenesis and to enhance LN and distant organ metastasis in various experimental mouse tumor models [20–24]. Conversely, the blocking of VEGF-C and VEGF-D from binding to VEGFR-3 inhibits these processes [22,25]. Reduced peritumoral lymphangiogenesis and LN metastasis have been demonstrated in *Vegfd*$^{-/-}$ mice in an orthotopic pancreatic tumor model [16], while the effect of VEGF-C deficiency on tumor growth is not known so far, due to embryonic lethality of the constitutive *Vegfc* deletion. Depending on the experimental model, human VEGF-D has been observed to either promote [22,24] or inhibit [23] angiogenesis and tumor growth. In a range of human cancers, the expression of VEGF-C or VEGF-D positively correlates with LN metastasis and with poor patient outcome [8,26,27]. Collectively these data indicate that both VEGF-C and VEGF-D may play major roles in tumor lymphangiogenesis and in metastatic spread to sentinel and distal LNs and beyond. Targeting these factors and their downstream signaling pathways could thus be a promising therapeutic strategy to prevent tumor progression and metastasis.

Although much is known about VEGFs in tumor growth and metastasis, the specific roles of VEGF-D in cutaneous cancers have not been studied previously. Here we investigated the effects of VEGF-D on the development and progression of skin tumors by subjecting both *Vegfd*$^{-/-}$ mice [15] and transgenic (TG) mice that overexpress mouse VEGF-D in the skin (keratin 14 [K14]-mVEGF-D mice) [28] to a two-stage chemical skin carcinogenesis model [29]. We show that while *Vegfd* deletion has rather marginal effects on skin tumor growth and lymphangiogenesis, TG overexpression of VEGF-D promotes tumor lymphangiogenesis and metastasis. Interestingly, VEGF-D also induces significant changes in immune cell and cytokine profiles in the developing skin tumors, leading to a shift from a protumoral Th2 to antitumoral Th1/Th17 response, and substantial regression of primary tumors in the K14-mVEGF-D mice.

Materials and Methods

Mice

Age- and sex-matched transgenic K14-mVEGF-D mice overexpressing mouse VEGF-D in the skin under the K14 promoter [Tg(KRT14-Figf)1Ali] [28] in the FVB/N background (TG) and VEGF-D knockout (KO) (Figf^{tm1Mach}) [15] mice, backcrossed into a FVB/N (Harlan, the Netherlands) background for at least five generations, were used for the skin carcinogenesis studies.

Chemical Skin Carcinogenesis

Each experimental group consisted of 15–30 TG, KO or wild type (WT) littermate control mice of 9–12 weeks of age. Mice were subjected to the chemical skin carcinogenesis involving 7,12-dimethylbenz[a]anthracene (DMBA; Sigma-Aldrich) and 12-*O*-tetradecanoyl phorbol-13-acetate (TPA; Sigma-Aldrich) treatments, and tumor development, size and, macroscopic appearance were monitored once a week for up to 30 weeks, as described earlier [30]. Mice were sacrificed at weeks 10, 15, 25, and 30, or at predetermined humane end points (engraved or ulcerative cSCCs, tumors with a diameter over 10 mm, or excessive tumor load per mouse). Tumor incidence (the percentage of mice with a tumor) and cumulative tumor multiplicity (the number of papillomas divided by the total number of mice alive at the time when the first mouse was removed from the experiment due to humane end points, as described by Abel et al. [29]) were recorded. To induce epidermal hyperplasia and chronic inflammation, the shaved dorsal skin of nine-week old mice was treated four times, at two-day intervals, with 5 μg of TPA in acetone and skin samples were collected on the ninth day from the first application. Mice treated with acetone were used as controls. Untreated dorsal skin was also collected from nine-week old mice. All the animal experiments were approved by the Finnish National Animal Experiment Board.

Tumor and Tissue Sample Harvesting

Mice were sacrificed by CO_2 inhalation and cervical dislocation; skin or skin tumors, and inguinal, axillary, and brachial lymph nodes were dissected. Tissue samples were either fixed in fresh phosphate-buffered 4% paraformaldehyde for 24 hours at 4 °C and embedded in paraffin or snap-frozen in liquid nitrogen. Hematoxylin-eosin-stained 5 μm sections from the subcapsular region of LNs were evaluated for the presence of metastases.

Histochemical and Immunohistochemical Analyses

Fixed tissue sections were: treated with trypsin for 30 min at 37 °C and stained with rat anti-mouse CD-31 antibody (BD Biosciences PharMingen) or rat anti-mouse VEGF-D antibody (ReliaTech); or heated in boiling EDTA-Tris buffer (pH 9.0) for 15 minutes and stained with rat anti-mouse monoclonal F4/80 antibody against macrophages (Serotec), rat anti-mouse CD45R antibody against B-lymphocytes (BD Biosciences) or rabbit anti-mouse VEGF-C antibody (Santa Cruz Biotechnology Inc.); or boiled in 10 mmol/L citrate buffer (pH 6.0) for 15 minutes and stained with goat anti-mouse VEGFR-3 antibody (R&D Systems) or rabbit anti-mouse LYVE-1 antibody [14]. The tyramide signal amplification kit (Perkin-Elmer) was used according to the manufacturer's instructions to intensify color reactions. A biotinylated anti-rat (Vector Laboratories), anti-rabbit (Jackson Immunoresearch), or anti-goat (R&D Systems) antibody was used as secondary antibody. A Histomouse-SP Broad Spectrum (AEC) kit was used to stain helper

T-cells with the monoclonal rat anti-mouse CD4 antibody (R&D Systems). Killer T-cells, lymphatic vessels and basement membranes were visualized by immunofluorescence staining using rat anti-mouse CD8 (R&D Systems), rabbit anti-mouse LYVE-1 [14], and rat anti-mouse laminin (Chemicon) antibodies, respectively, followed by appropriate secondary antibodies conjugated with Cy-2 or Cy3 (Jackson Immunoresearch). Cell nuclei were labeled with DAPI (Sigma-Aldrich). Mast cells were visualized by Leder's method of chloroacetate esterase histochemistry [31].

The Quantitation of Vessels and Immune Cells

Intratumoral blood vessels and peritumoral lymphatic vessels were counted at 200x magnification from 4 to 10 microscopic fields representing the areas of highest vascular density. Branching structures were considered as a single vessel. The number of various inflammatory cell types was counted at 200x magnification from 4 to 6 random fields representing the areas of the highest density of immune cells within the tissue section. In each time point, 4 to 15 papillomas collected from 3 to 11 individual mice/genotype, and 2 to 10 cSCCs collected from 2 to 10 individual mice/genotype were used for quantification. Vessels and immune cells in untreated skin (WT = 10, TG = 7) and TPA-treated skin (WT = 6, TG = 6) were counted at same magnification from 4 to 10 random fields.

Quantitative Real-Time PCR (qPCR)

Total RNA was extracted from untreated skin, TPA-treated skin, and skin tumors using TriPure reagent (Sigma-Aldrich) according to the manufacturer's instructions. In each time point or group, RNAs from at least 5 samples collected from at least 5 individual mice/genotype were pooled for qPCR analysis. A total of 0.5 μg of RNA was used to synthesize cDNA using an iScript cDNA Synthesis Kit (BioRad). The PCR primers for mouse interleukin (IL)-1β, IL-2, IL-4, IL-6, IL-10, IL-12, IL-17A, IL-17 F, IL-23p19, interferon (IFN)-γ, transforming growth factor (TGF)-β, tumor necrosis factor (TNF)-α, and β-actin were obtained from published studies [32–38]. The primers for the M2 macrophage marker MRC1/CD206 were 5'-TCGGTGGACTGTGGACGAGCA (sense) and 5'-TCCCGCCTTTCGTCCTGGCA (antisense), and for the M1 macrophage marker CD11c/ITGAX 5'-AGCCTTTCT TCTGCTGTTGGGGT (sense) and 5'-TGTCCGAACTCAG-CACCGTCCA (antisense). qPCR was performed with iTaq SYBR Green Supermix with ROX reagents (BioRad). Each sample was run in duplicate or triplicate using a Mx3005P qPCR device (Stratagene), and repeated at least three times. Relative RNA levels were calculated by the $2^{\Delta\Delta Ct}$ method [39]. Values were normalized against β-actin, and the control values (the untreated skin of the WT mice) were expressed as 1 to indicate a precise fold change.

Fluoresence-Activated Cell Sorting (FACS)

Mouse skin (WT = 6, TG = 5) with emerging papillomas was removed at week 10 after DMBA and TPA treatments, cut into small pieces, digested with collagenase (Worthington) for 2–3 h at 37 °C, washed and resuspended in PBS, and filtered through a 40-μm mesh to obtain single cell suspension. Cells were first stained for cell-surface markers, then fixed and permeabilized with Cytofix/Cytoperm (BD Biosciences) and stained for different intracellular cytokines according to the manufacturer's instructions. The following antibodies were used: fluorescent anti-CD3, CD4, CD8a, CD11b, Ly-6G/C (Gr-1), F4/80, TNF-α, IFN-γ, IL-4, and IL-6 (all from BD Biosciences). Isotype-matched antibodies were routinely used for background correction. Phenotypic populations were defined as follows: $CD4^+$ T helper cells ($CD3^+CD4^+Gr\text{-}1^-$), $CD8^+$ cytotoxic T-cells ($CD3^+CD8^+Gr\text{-}1^-$), and macrophages ($Gr\text{-}1^-CD11b^+F4/80^+$). Samples were analyzed in duplicate on a FACSCalibur cytometer running CellQuest software (BD Biosciences). Values reported are given as a percentage of each immune subpopulation of total cells acquired (for immune cells) or as mean fluorescence intensity (for cytokines).

Statistical Analysis

For most of the experiments, a two-tailed unpaired *t* test was used. When more than two groups were considered (IFN-γ, TNF-α, and IL-4), a non-parametric Kruskal-Wallis test, followed by a Dunn post-hoc test, was used. Differences in metastasis formation were assessed using the χ^2 test. In all cases, differences were considered significant at $P < .05$, and values are presented as mean ± SD.

Results

Skin Tumor Formation is Impaired in K14-mVEGF-D Mice

To explore the *in vivo* role of VEGF-D in skin carcinogenesis we first compared the development and progression of chemical-induced skin tumors between TG K14-mVEGF-D mice and WT control mice (Figure 1, Supplementary Figure S1; the combined data of two separate experimental groups is presented in both figures). We observed a significant delay in tumor incidence (i.e. the proportion of mice bearing at least one tumor) from week six up to week 13 in the TG mice in comparison to the controls ($P < .01$-$.001$; Figure 1*B*; Supplementary Figures S1*A* and S1*C*). The delay was the most prominent in male mice at week seven when only 12% of the TG males had developed papillomas in comparison with 52% of the WT males ($P < .001$) (Figure 1*B*). Moreover, the TG mice developed markedly fewer papillomas than the WT mice (Figure 1*A* and *C*, Supplementary Figures S1*B* and S1*D*). The differences in papilloma numbers were already evident at week 7 ($P < .01$), and from week 13 onwards the TG males showed approximately 40% less papillomas than the WT males ($P < .001$). The third experimental group was followed until week 14, when the rate of tumor development was comparable to that of the 2 other groups, the TG mice having significantly less papillomas than the WT mice from week 8 onwards ($P < .05$-$.001$) (not shown). In females tumor multiplicity showed a similar trend between the genotypes, but the variation between individuals was greater and statistical significance was reached mainly at late time points (Supplementary Figure S1*B*).

Upon tumor monitoring, visual inspection revealed a bigger proportion of regressing papillomas in the TG mice in comparison with the controls ($P < .05$-$.001$ from week 14 onwards) (Figure 1*D*). Differing from typical exophytic pedunculated papillomas of the WT mice, the appearance of these lesions in the TG mice was sessile, often slightly scaly, and many of them disappeared gradually (Figure 1*A*). Only few regressed-like lesions could be found in the TG mice after 25 weeks, and the skin looked healthy around the remaining and growing tumors (Figure 1*A*).

The monitoring of a large number of skin tumors revealed a difference in tumor size between the TG and WT mice. The proportion of papillomas over 2 mm in diameter was significantly lower in the TG mice compared to the WT mice ($P < .001$ at weeks 10, 15, and 20) (Figure 1*E* and Supplementary Table S1). Relative to the controls, the proportion of big tumors (over 6 mm in diameter) was also clearly lower in the TG mice in the late stages of skin carcinogenesis ($P < .001$ at weeks 20 and 25).

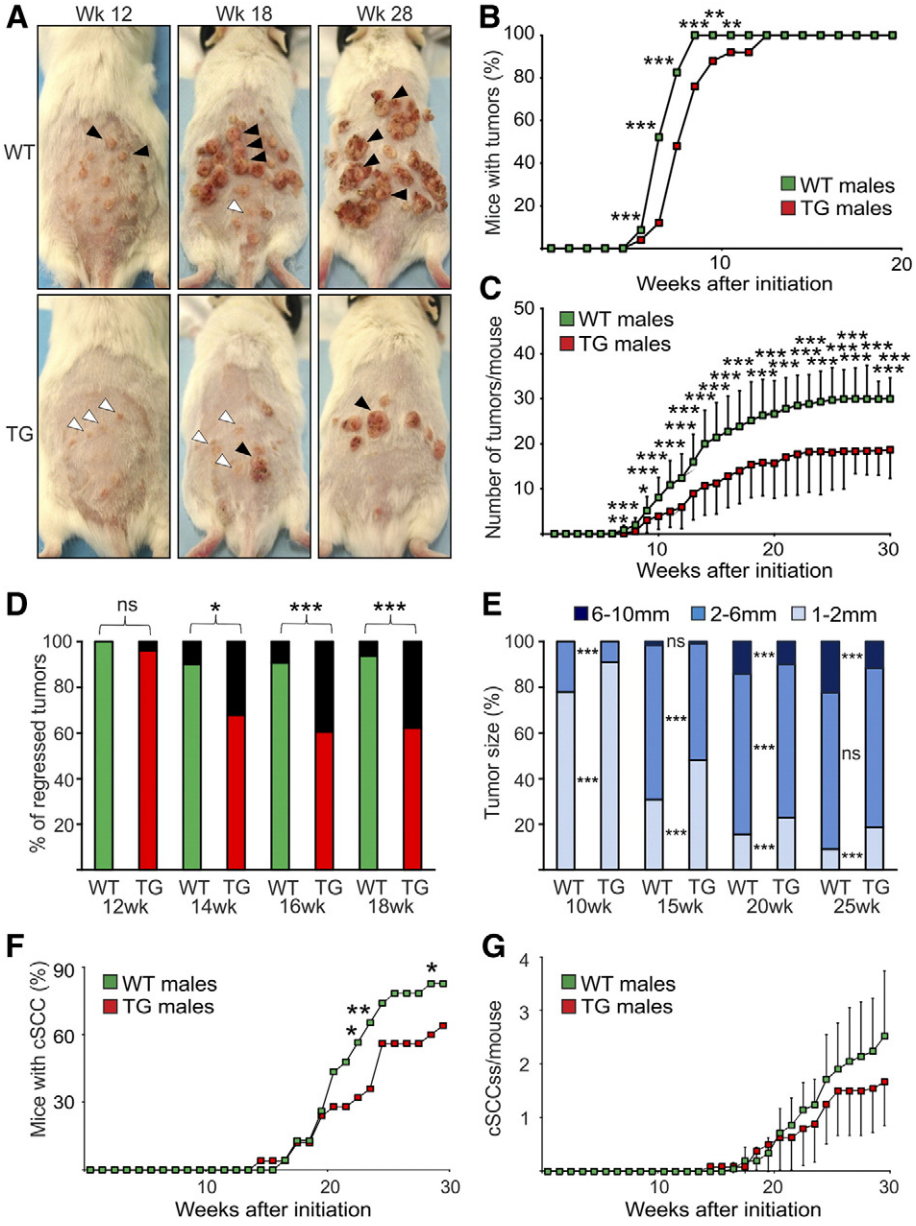

Figure 1. Impaired skin tumor formation in TG K14-mVEGF-D mice in a chemical skin carcinogenesis model. Tumors were induced in the mouse skin using a multistage DMBA-TPA protocol and their growth was monitored for up to 30 weeks (Wk). Data from two separate experimental groups of males (WT N = 23, TG N = 25) are combined. (A) Representative photographs of the WT and K14-mVEGF-D TG male mice at different time points. Black arrowheads indicate exophytic papillomas and white arrowheads regressing papillomas. (B) Tumor incidence showed a significant delay in the TG mice. (C) The TG mice developed markedly less tumors than the WT mice. Cumulative tumor multiplicity is shown. (D) The percentage of regressing papillomas (the black portion of the column) was higher in the TG mice (red) than in the WT mice (green). (E) Smaller tumor size in the TG mice than in the WT mice. Tumor sizes are shown as a percentage of tumors in three different size categories. Statistical significance for each size category is shown in between the column pairs. (F) At weeks 20–30 the percentage of TG male mice with clinically apparent cSCC was lower than that of WT control males. (G) A trend towards less cSCCs per mouse was observed in TG males. N = number of mice. Error bars: SD.*: $P < .05$; **: $P < .01$; ***: $P < .001$; ns: not significant.

We also scored the progression of papillomas to cSCCs, which typically appear as endophytic, often doughnut-shaped tumors with erosion or ulceration (Supplementary Figure S1*E*). There was a trend for lower cSCC incidence in the TG mice than in the WT mice, and at weeks 23, 24, and 29 this difference was also statistically significant ($P < .05$-$.01$) (Figure 1*F*). Even though statistically significant differences were not observed in the cSCC multiplicity between the genotypes, we found a trend towards less carcinomas per mouse in the K14-mVEGF-D group than in the control group (Figure 1*G*).

Deletion of *Vegfd* in mice had no significant effects on skin tumor growth; nevertheless, the KO males showed a slight trend of more papillomas and cSCCs per mouse than their WT male littermates (Figure 2 and Supplementary Figure S2; the combined data of two separate experimental groups is presented in both figures). Immunohistochemistry revealed that in the WT mouse tumors, VEGF-D was expressed in the stromal compartment by macrophages, and in some cSCCs also by invasive tumor cells, while sections from the KO tumors were negative for VEGF-D staining (Figure 2, *C* and *D*).

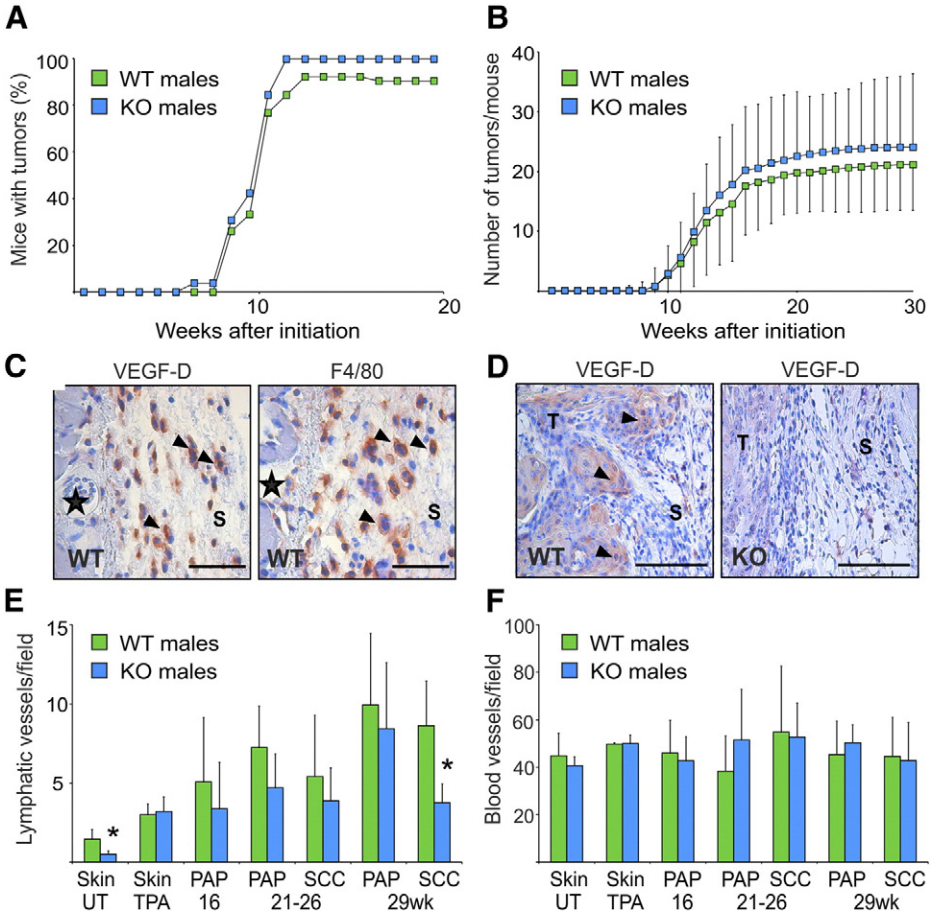

Figure 2. DMBA-TPA-induced skin carcinogenesis in VEGF-D knockout mice. Tumor incidence (A) and cumulative multiplicity (B) in the KO males (N = 26) and the WT males (N = 27) did not show statistically significant differences between the genotypes. (*C-D*) Expression of VEGF-D in mouse skin tumors. Representative immunohistochemical stainings showing VEGF-D expression in mouse cSCCs. (C) Consecutive sections of the WT cSCC stained with antibodies against VEGF-D and F4/80 demonstrate that VEGF-D is expressed by F4/80-positive macrophages (arrowheads) within the WT cSCC stroma. Asterisks indicate vessels that facilitate the identification of co-stained cells in the consecutive sections. (D) VEGF-D expression by invasive carcinoma cells (arrowheads) within the WT cSCC. The KO cSCC is used as a negative control for VEGF-D staining. (E) The quantification of lymphatic vessel density in the untreated (UT) skin, TPA-treated skin, and papillomas (PAP) and cSCCs collected at different time points of skin carcinogenesis. The KO tumors showed a trend for reduced lymphangiogenesis. In the UT skin, and in cSCCs at week 29, the difference between the genotypes was significant. (F) No significant differences in blood vessel densities between the KO and WT males in any type of sample. Scale bars: 50 μm (C) and 100 μm (D): Error bars: SD. *: $P < .05$.

Collectively, our data imply that high VEGF-D expression in the mouse skin markedly impairs tumor development in the chemical skin carcinogenesis model.

Elevated VEGF-D Leads to an Increase in Tumor Lymphangiogenesis and in LN Metastasis

VEGF-D acts as a ligand for VEGFR-3, and signaling through this receptor can activate both tumor lymphangiogenesis and angiogenesis [18]. The number of peritumoral LYVE-1-positive lymphatic vessels was significantly higher in the TG mice than in WT mice at various stages of skin tumorigenesis (papillomas at weeks 10, 15, and 20–24 [$P < .05$], and cSCCs at week 30 [$P < .05$]) (Figure 3*A* and *B;* Supplementary Figure S*3*). The lymphatic vessel density was also about two times higher in the untreated TG skin in comparison with the control skin ($P < .05$), and strongly increased in the dermis of mutant mice versus controls in TPA-induced skin hyperplasia ($P < .001$). In contrast, the papillomas and cSCCs in the KO mice showed a trend towards decreased tumor lymphangiogenesis, and in the untreated skin and in cSCCs at week 29, the difference between genotypes was also statistically significant ($P < .05$) (Figure 2*E*). Relative to the WT mice, skin tumor angiogenesis showed no differences in the TG mice (Figure 3*C* and *D*) or KO mice (Figure 2*F*).

Metastatic dissemination into regional LNs was increased in the TG mice relative to the WT mice at late time points (Figure 3*E*) but not affected in the KO mice (Supplementary Figure S2*C*). At weeks 26–30 the frequency of LN metastasis in the cSCC-bearing TG mice was even 60% in comparison with 29% in the WT mice ($P < .05$; Figure 3*E*). These data show that VEGF-D induces lymphangiogenesis in mouse skin tumors and promotes tumor metastatic spread at the late stage of skin carcinogenesis, supporting the previous observations from other tumor models [22–24].

Altered Immune Response in the Skin Tumors of the K14-mVEGF-D Mice

In order to explain the distinctly enhanced papilloma regression in the K14-mVEGF-D mice, we next focused on tumor inflammation. Immunohistochemical analysis demonstrated markedly less $CD4^+$

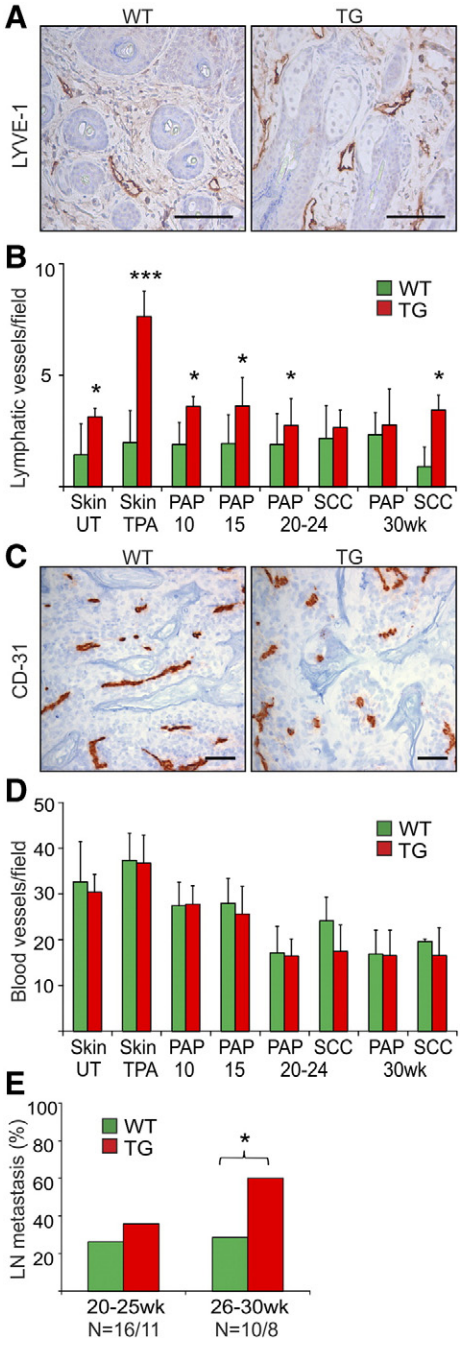

Figure 3. Increased tumor lymphangiogenesis and lymph node metastasis in TG K14-mVEGF-D mice. (A) Representative images of peritumoral LYVE-1 immunohistochemistry in WT and TG papillomas at week 20. (B) The quantification of lymphatic vessel density in the UT skin, TPA-treated skin, and PAPs and cSCCs collected at different time points. Tumor lymphangiogenesis was more prominent in the TG mice than in the WT mice. (C) Representative images of intratumoral CD-31 immunohistochemistry in WT and TG papillomas at week 20. (D) No significant differences in blood vessel densities between the TG and WT mice in any type of sample. (E) The frequency of LN metastasis at weeks 26–30 was significantly higher in the TG mice than in the WT mice. Scale bar: 100 μm. Error bars: SD. *: $P < .05$; ***: $P < .001$.

T-helper cells within TG tumor stroma relative to WT stroma (Figure 4, *A* and *B,* and not shown). This difference was already seen from week 10 onwards and was significant in all stages of skin carcinogenesis ($P < .05$ to 0.01). On the contrary, the number of $CD8^+$ cytotoxic T-cells was prominently increased in TG papillomas at weeks 20–24 ($P < .01$) and at week 30 ($P < .05$) in comparison with WT papillomas (Figure 4, *C* and *D*). We also found a significant decrease in $F4/80^+$ macrophage accumulation in the TG papillomas and cSCCs at weeks 20–25 ($P < .05$–0.01) (Figure 4, *E* and *F)*, and also less Leder-positive mast cells in the TG papillomas (a significant difference at week 30 [$P < .05$]) (Supplementary Figures S4*A* and S4*B*). FACS analysis corroborated our findings on significantly less macrophages and $CD4^+$ T-cells, and more $CD8^+$ T-cells at the early stage of skin tumorigenesis (week 10) (Figure 4G and Supplementary Figure S5). Immune cells counts were comparable in the untreated and TPA-treated skin of the TG and WT mice (Figure 4). No differences were detected in macrophage, mast cell or $CD4^+$ T-cell counts between the KO and WT tumors nor in the TPA-treated or untreated skin (Supplementary Figures S4*C*-S4*E*).

VEGF-D Modulates Immune Cell Polarization in Skin Tumors

Depending on microenvironmental signals, macrophages polarize to either anti-tumoral (M1) or pro-tumoral (M2) phenotypes, and $CD4^+$ T cells differentiate into various T helper (Th) cell lineages cells with distinct functions in tumor immunity [40,41]. Simplifying, the interferon-γ (INF- γ) –producing Th1 subset possesses tumor cell cytotoxicity and also polarizes macrophages towards M1 phenotype, while interleukin-4 (IL-4) –producing Th2 cells stimulate alternative M2 activation program and oppose antitumor responses. Finally, the roles of IL-17 -producing Th17 subsets in tumors are more complex and still controversial [40,42].

To evaluate whether VEGF-D production could alter immune cells polarization during carcinogenesis, we performed qPCR to compare cytokine levels in total RNA fractions extracted from healthy skin, TPA-treated skin, and skin tumors collected at different time points. These data suggested changes in cutaneous cytokine levels between the TG and WT samples, showing, for example, that the upregulation of IL-4 mRNA (a typical pro-tumoral cytokine) was significantly lower in TPA-treated hyperplastic skin and the skin tumors of the TG mice in comparison to their WT littermates ($P < .05$ in papillomas at week 15, and $P < .01$ in cSCCs at weeks 20–24) (Figure 5*A*), possibly indicating a role for VEGF-D in Th1 polarization. Accordingly, the typical M1 biomarkers IL-1β, IL-6, and IL-12 mRNAs were significantly higher in the untreated TG skin in comparison with the WT skin ($P < .05$) (Figure 5*B*) suggesting the predisposition of the TG skin towards Th1 responses. During skin carcinogenesis, however, their expression levels varied depending on the time point and the genotype (not shown).

As the Th17 cells are known to develop from naïve $CD4^+$ T cells in the presence of at least IL-6 and IL-1β and are maintained by IL-23 [41,42], we sought to investigate whether the Th1 predisposition of TG mice would lead to differences in Th17 responses during experimental skin carcinogenesis. We found that while IL-17A and IL-17 mRNAs were either undetectable or expressed at very low levels in all WT samples and in the healthy TG skin, they strongly peaked in TG papillomas at week 15 ($P < .001$ for both cytokines), rapidly dropping down at later stages of papilloma and cSCC development (Supplementary Figures S6*A* and S6*B*). Similarly, IL-23 expression reached significantly higher levels in TG papillomas at week 15 in respect to WT papillomas ($P < .01$), and then decreased to WT control levels, though with a slower pace than IL-17A and IL-17 F (Supplementary Figure S6*C*). No obvious differences were observed

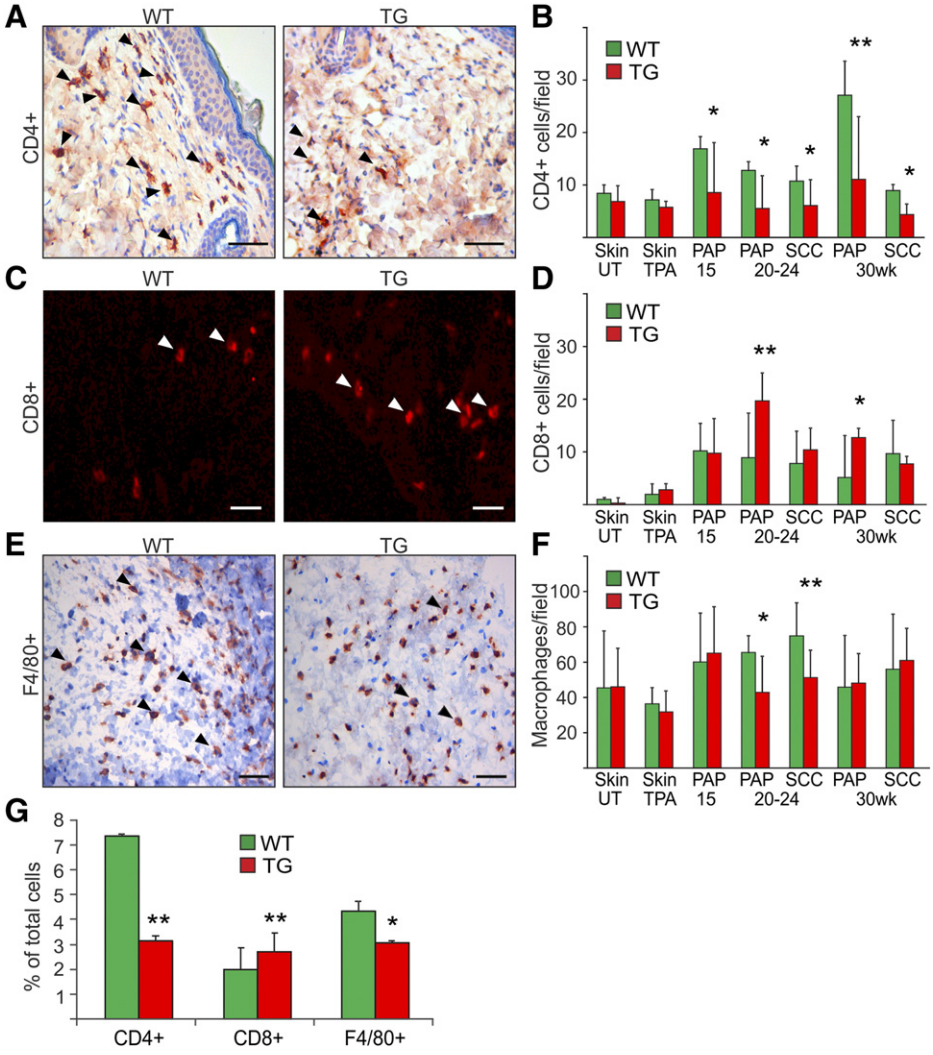

Figure 4. The TG overexpression of VEGF-D affects inflammatory cell accumulation in skin tumors. Representative photographs of $CD4^+$ (A) and $CD8^+$ (C) T-cells and $F4/80^+$ macrophages (E) in the peritumoral area of WT and TG papillomas at week 20. The number of $CD4^+$ (B) and $CD8^+$ T-cells (D), and macrophages (F) in the UT skin, TPA-treated skin, PAPs and cSCCs collected at different time points of skin carcinogenesis. VEGF-D overexpression resulted in significantly less $CD4^+$ T-cells and macrophages, and more $CD8^+$ T-cells in skin tumors at several time points of skin carcinogenesis. (G) FACS analysis revealed significantly less $CD4^+$ T-cells ($CD3^+CD4^+Gr\text{-}1^-$) and macrophages ($Gr\text{-}1^-CD11b^+F4/80^+$), and significantly more $CD8^+$ T-cells ($CD3^+CD8^+Gr\text{-}1^-$) in the DMBA-TPA treated skin of the TG mice (N = 5) than in the WT mice (N = 6) at week 10 of carcinogenesis. Scale bars: 100 μm (A, E) and 50 μm (C). Error bars: SD. *: $P < .05$; **: $P < .01$.

in IFN-γ, IL-2, IL-10, TGF-β, TNF-α, MRC1/CD206, or CD11c mRNA levels between the TG and WT mice (not shown). Altogether, the cytokine expression profiles suggested that experimental overexpression of VEGF-D primes mouse skin towards a Th1/M1 phenotype, which favors the onset of strong Th17 response during early phase of tumorigenesis.

To further verify the effects of VEGF-D on the polarization of immune cells, we quantified key pro- and anti-tumoral cytokines by intracellular staining and FACS analysis. After 10 weeks of DMBA and TPA treatments, a significant polarization towards the production of inflammatory cytokines (TNF-α and IL-6 in macrophages and TNF-α in T-cells) could be observed in the TG samples in comparison to the WT samples (Figure 5, *C* and *D*; Supplementary Figure S7), again suggestive of the anti-tumoral M1/Th1 polarization due to VEGF-D overexpression. Likewise, IFN-γ (another prototypical Th1 cytokine) was significantly elevated in T-cells and the macrophages of the TG tumors in comparison with those of the WT tumors (Figure 5*E* and Supplementary Figure S7). Differing from lower total IL-4 mRNA in TG skin relative to WT skin (Figure 5*A*), its level was higher in the immune cells of the TG mice than in those of the WT mice (Figure 5*F* and Supplementary Figure S7). Collectively, these data suggest that, in early skin tumorigenesis, elevated VEGF-D attenuates Th2 polarization in favor of a more robust Th1 response. This, in turn, could significantly reduce and delay tumor growth and burden.

Discussion

The most striking observation in this study was the inhibitory effect of VEGF-D overexpression on primary skin tumor growth. A comparable finding has been made previously in a Rip1Tag2 mouse model of pancreatic cancer wherein overexpression of VEGF-D in β-cells resulted in reduced tumor outgrowth [23]. In our study, the number and size of the DMBA-TPA-induced skin tumors were significantly decreased and their incidence delayed in the TG

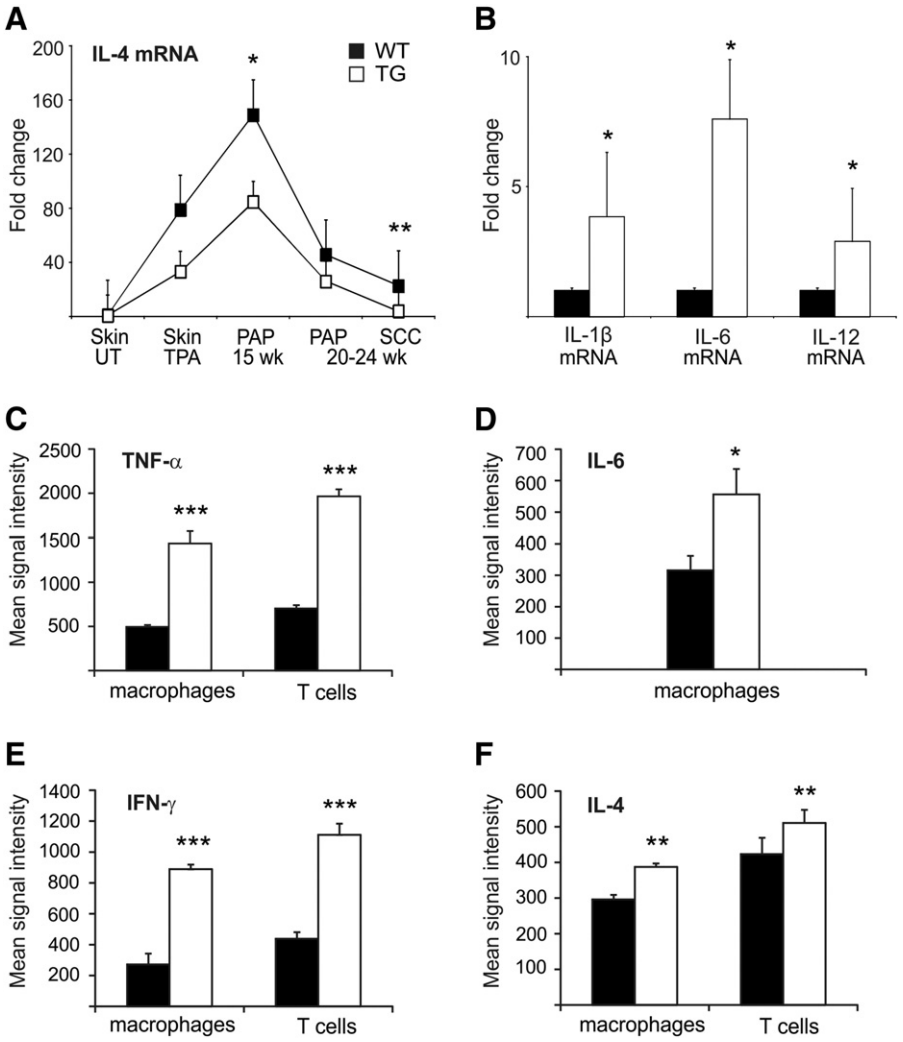

Figure 5. VEGF-D affects immune cell polarization. Cytokine expression in the skin and skin tumors of the K14-mVEGF-D TG mice and WT mice. Analyses using qPCR were carried out with total RNA isolated from the UT skin and PAPs collected from the TG mice (white) and WT mice (black) at different time points during skin tumorigenesis. (A) Interleukin IL-4 mRNA levels were lower in the TG tumors than in the WT tumors. (B) IL-1β, IL-6 and IL-12 mRNAs were upregulated in the UT TG skin when compared with the UT WT skin. (*C-F*) FACS profiling of key cytokines in macrophages and T-cells at week 10 of skin tumorigenesis. Relative to the WT mice (N = 6), the TG mice (N = 5) show a robust Th1 response and polarization towards the M1 phenotype, evidenced by higher levels of anti-tumoral TNF-α (C), IL-6 (D), and IFN-γ (E), and pro/anti-tumoral IL-4 (D). Error bars: SD. *: $P < .05$; **: $P < .01$; ***: $P < .001$.

K14-mVEGF-D mice in comparison with the controls. VEGF-D or VEGF-C do not appear to affect keratinocyte proliferation or survival [43], implying that these factors rather have an indirect influence on primary tumor growth.

Inflammation plays a critical role in tumorigenesis and can either promote or suppress tumor growth [40,41]. We found that in the two-stage skin carcinogenesis model, VEGF-D attenuates the Th2 response that normally boosts tumor development via induction of chronic inflammation. This was evidenced by an increase in the amount of cytotoxic $CD8^+$ T-cells and a concomitant decrease in $CD4^+$ T-cells, macrophages, and mast cells in VEGF-D overexpressing tumors. Mice lacking $CD4^+$ T-cells show reduced tumor incidence and number, and delayed neoplastic progression in experimental skin cancer, while in the CD8 KO mice, tumor development is enhanced [44,45]. Moreover, human cSCC patients with a high amount of peritumoral $CD8^+$ T-cells tend to survive longer and have a lower neoplastic cell proliferation index [46].

FACS analysis of intracellular cytokines in tumor macrophages and T-cells demonstrated that TNF-α, IFN-γ, and IL-6 were significantly higher in early stage papillomas of the TG mice rather than the WT mice, indicating that VEGF-D promotes anti-tumoral M1/Th1 polarization. qPCR revealed high expression of typical Th17 response markers in early stage TG papillomas relative to WT papillomas, too. Th17 cells have both pro- and antitumorigenic effects [42], but, based on our data on significantly less primary skin tumors and elevated M1/Th1 response in the excess of VEGF-D, we believe the observed Th17 activation is aimed towards tumor rejection. However, it should be kept in mind that strict classification of immune responses to anti-tumoral M1/Th1 and pro-tumoral M2/Th2 categories simplifies the situation prevailing in tumor tissues, and immune cells rather show considerable heterogeneity as pointed out recently for macrophage populations in human cSCC [47].

Unexpectedly, IL-4 was also higher in TG immune cells than in WT immune cells, but its transcript was constantly lower in the total

RNA pool extracted from papillomas and cSCCs. IL-4 is one of the key pro-tumoral cytokines that supports Th2 activation in an autocrine manner, induces alternative activation of macrophages, and downregulates Th1 responses [48]. It should be noted, however, that IL-4 also has anti-tumoral effects – such as the recruitment and activation of innate immune cells and the enhancement of $CD8^+$ T-cell mediated anti-tumor immunity – and that its diverse effects in tumors seem to depend on source and target cells, concentration, and expression kinetics, as well as on its interaction with multiple microenvironmental factors [49].

A significant up-regulation of the M1 macrophage markers IL-1β, IL-6, and IL-12 was also observed in the untreated TG skin in comparison with the WT skin, while in tumors their levels were comparable between the genotypes. These observations suggest a selective skewing of the skin immune environment to favor a M1 phenotype in the untreated TG skin, and a role of VEGF-D in shaping the immune environment of healthy mouse skin towards an anti-tumoral setup that preserves the anti-tumoral polarization of tumor macrophages and T-cells, thus leading the regression of primary tumors in the TG mice.

Interestingly, a recent study showed that VEGF-D induces and a VEGFR-3 neutralizing antibody suppresses the production of IL-6 by $CD11c^+$ dendritic cells and results in enhanced anti-tumor immunity in an allogeneic hematopoietic stem cell transplantation model in mice, thus endorsing our view about the immunomodulative role of the VEGF-D/VEGFR-3 axis [50]. Moreover, transgenic delivery of VEGF-C or VEGF-D was shown to ameliorate the persistent chronic inflammation in the oxazolone-treated skin of K14-VEGF-A mice, implying that functional lymphatic vessels activation via VEGFR-3 functions in preventing the development of chronic inflammation [51].

The importance of properly regulated VEGFR-3 signaling in tumor inflammation is further supported by another recent study wherein the blocking of VEGF-C and VEGF-D by the transgenic overexpression of soluble VEGFR-3 (sVEGFR-3) inhibited the development of a pro-tumorigenic tissue microenvironment, leading to decreased skin tumor growth in the DMBA-TPA model [43]. Consistent with our study, the amounts of macrophages and $CD4^+$ T-cells were significantly lower in the sVEGFR-3 TG skin, however, changes in macrophage polarization were not observed. Decreases in $CD45^+$ leukocytes and $F4/80^+$ macrophages, as well as the reduced growth of pancreatic tumors, were also observed in the Rip1Tag2 model upon VEGF-D overexpression [23], further highlighting VEGF-D/VEGFR-3 signaling in modulating a tumor immune environment. The opposite to these findings (an increased number of macrophages and accelerated tumor growth) was observed in a human xenograft model upon VEGF-D overexpression [24], but the use of an immunodeficient host in this model makes it difficult to compare the data with our immunocompetent model. Hence, both sequestering of VEGF-C and VEGF-D, and overexpression of VEGF-D appear to entangle VEGFR-3 signaling in the mouse skin, resulting in an anti-tumorigenic inflammatory microenvironment; however, the detailed molecular mechanisms behind these observations are still obscure.

Lymphangiogenesis is elevated in various cutaneous tumors and correlates with the incidence of early sentinel LN metastasis and reduced survival rates [7,52]. We show here that overexpression of VEGF-D leads to higher lymphatic vessel densities in healthy mouse skin, in chronically inflamed skin, and in carcinogen-induced skin tumors and enhances the spread of cancer cells to sentinel LNs. These observations are consistent with previous mouse and human data [16,23,24,26–28]. Interestingly, it was recently shown that Th17-secreted IL-17 can directly induce VEGF-D expression and corneal lymphangiogenesis in mice [53]. We observed here both high IL-17 levels and elevated lymphangiogenesis in early stage skin tumors of K14-mVEGF-D overexpressing mice. Even if we did not study the relationship between VEGF-D and IL-17 at molecular level, the observations by Chauhan et al. and us may imply a crosstalk between the two growth factors in regulating lymphangiogenesis. In an opposite result to previous studies [15,16], we detected reduced lymphatic vessel density in the healthy skin of the *Vegfd*-deleted mice. A lack of VEGF-D has been shown to dampen lymphagiogenesis and metastasis in an orthotopic pancreatic tumor model [16], and we also found a trend for reduced lymphangiogenesis in the KO papillomas and cSCCs, albeit with no observed effects on LN metastasis. It should be noted, however, that the rate of metastasis of experimental skin tumors is generally low, and also the DMBA-TPA protocol is of limited utility for studying metastasis [29]. Likewise in human [7], murine VEGF-D expression was detected in inflammatory cells adjacent to the cSCC, and in invasive cancer cells, suggesting that it is up-regulated upon malignant conversion, and contributes to tumor lymphangiogenesis.

In conclusion, our data imply that aberrant regulation of VEGFR-3 signaling due to elevated of VEGF-D in the mouse skin has two outcomes: first, the beneficial modulation of the inflammatory tissue microenvironment, which shifts intratumoral immune responses away from a tumor-supportive Th2-type and towards a tumor-suppressive Th1/Th17-type, and substantial regression of primary skin tumors in an early stage of carcinogenesis; and second, the prejudicial stimulation of lymphangiogenesis, which raises the frequency of LN metastasis. While high VEGF-D levels in human tumors generally correlates positively with increased metastasis and reduced survival [8,26,27], and with poor differentiation and increased invasiveness [54,55], correlations with a good prognosis and high differentiation grade have also been presented recently [56].

Acknowledgments

We thank: Maija Seppänen, Jaana Peters, and Päivi Tuomaala for their excellent technical assistance, and Dr. Mari Aikio for help with qPCR; Dr. Steven Stacker and Dr. Marc Achen of the University of Melbourne, for providing the VEGF-D KO mice for this study; the personnel of the Laboratory Animal Centre at the University of Oulu and Transgenic Core Facility at Biocenter Oulu for help with all mouse work; and Dr. Markus J. Mäkinen and Riitta Vuento of the Department of Pathology of the University of Oulu, for help with the immunohistochemical staining and analysis.

Appendix A. Supplementary data

Supplementary data to this article can be found online at http://dx.doi.org/10.1016/j.neo.2016.05.002.

References

[1] Alam M and Ratner D (2001). Cutaneous squamous-cell carcinoma. *N Engl J Med* **344**, 975–983.

[2] Kivisaari A and Kähäri VM (2013). Squamous cell carcinoma of the skin: emerging need for novel biomarkers. *World J Clin Oncol* **4**, 85–90. http://dx.doi.org/10.5306/wjco.v4.i4.85.

[3] Madan V, Lear JT, and Szeimies RM (2010). Non-melanoma skin cancer. *Lancet* **375**, 673–685. http://dx.doi.org/10.1016/S0140-6736(09)61196-X.

[4] Fu J, Bassi DE, Zhang J, Li T, Cai KQ, Testa CL, Nicolas E, and Klein-Szanto AJ (2013). Enhanced UV-induced skin carcinogenesis in transgenic mice overexpressing proprotein convertases. *Neoplasia* **15**, 169–179.

[5] Weinberg AS, Ogle CA, and Shim EK (2007). Metastatic cutaneous squamous cell carcinoma: an update. *Dermatol Surg* **33**, 885–899.

[6] Edge SB and Compton CC (2010). The American Joint Committee on Cancer: the 7th edition of the AJCC cancer staging manual and the future of TNM. *Ann Surg Oncol* **17**, 1471–1474. http://dx.doi.org/10.1245/s10434-010-0985-4.

[7] Moussai D, Mitsui H, Pettersen JS, Pierson KC, Shah KR, Suárez-Fariñas M, Cardinale IR, Bluth MJ, Krueger JG, and Carucci JA (2011). The human cutaneous squamous cell carcinoma microenv ironment is characterized by increased lymphatic density and enhanced expression of macrophage-derived VEGF-C. *J Invest Dermatol* **131**, 229–236. http://dx.doi.org/10.1038/jid.2010.266.

[8] Tobler NE and Detmar M (2006). Tumor and lymph node lymphangiogenesis - impact on cancer metastasis. *J Leukoc Biol* **80**, 691–696.

[9] Ruddell A, Harrell MI, Furuya M, Kirschbaum SB, and Iritani BM (2011). B lymphocytes promote lymphogenous metastasis of lymphoma and melanoma. *Neoplasia* **13**, 748–757.

[10] Joukov V, Pajusola K, Kaipainen A, Chilov D, Lahtinen I, Kukk E, Saksela O, Kalkkinen N, and Alitalo K (1996). A novel vascular endothelial growth factor, VEGF-C, is a ligand for the Flt4 (VEGFR-3) and KDR (VEGFR-2) receptor tyrosine kinases. *EMBO J* **15**, 290–298.

[11] Achen MG, Jeltsch M, Kukk E, Mäkinen T, Vitali A, Wilks AF, Alitalo K, and Stacker SA (1998). Vascular endothelial growth factor D (VEGF-D) is a ligand for the tyrosine kinases VEGF receptor 2 (Flk1) and VEGF receptor 3 (Flt4). *Proc Natl Acad Sci U S A* **95**, 548–553.

[12] Mäkinen T, Veikkola T, Mustjoki S, Karpanen T, Catimel B, Nice EC, Wise L, Mercer A, Kowalski H, and Kerjaschki D, et al (2001). Isolated lymphatic endothelial cells transduce growth, survival and migratory signals via the VEGF-C/D receptor VEGFR-3. *EMBO J* **20**, 4762–4773.

[13] Tammela T, Zarkada G, Wallgard E, Murtomäki A, Suchting S, Wirzenius M, Waltari M, Hellström M, Schomber T, and Peltonen R, et al (2008). Blocking VEGFR-3 suppresses angiogenic sprouting and vascular network formation. *Nature* **454**, 656–660. http://dx.doi.org/10.1038/nature07083.

[14] Kärkkäinen MJ, Haiko P, Sainio K, Partanen J, Taipale J, Petrova TV, Jeltsch M, Jackson DG, Talikka M, and Rauvala H, et al (2004). Vascular endothelial growth factor C is required for sprouting of the first lymphatic vessels from embryonic veins. *Nat Immunol* **5**, 74–80.

[15] Baldwin ME, Halford MM, Roufail S, Williams RA, Hibbs ML, Grail D, Kubo H, Stacker SA, and Achen MG (2005). Vascular endothelial growth factor D is dispensable for development of the lymphatic system. *Mol Cell Biol* **25**, 2441–2449.

[16] Koch M, Dettori D, Van Nuffelen A, Souffreau J, Marconcini L, Wallays G, Moons L, Bruyère F, Oliviero S, and Noel A, et al (2009). VEGF-D deficiency in mice does not affect embryonic or postnatal lymphangiogenesis but reduces lymphatic metastasis. *J Pathol* **219**, 356–364. http://dx.doi.org/10.1002/path.2605.

[17] Paquet-Fifield S, Levy SM, Sato T, Shayan R, Karnezis T, Davydova N, Nowell CJ, Roufail S, Ma GZ, and Zhang YF, et al (2013). Vascular endothelial growth factor-d modulates caliber and function of initial lymphatics in the dermis. *J Invest Dermatol* **133**, 2074–2084. http://dx.doi.org/10.1038/jid.2013.83.

[18] Alitalo K (2011). The lymphatic vasculature in disease. *Nat Med* **17**, 1371–1380. http://dx.doi.org/10.1038/nm.2545.

[19] Baldwin ME, Catimel B, Nice EC, Nice EC, Roufail S, Hall NE, Stenvers KL, Kärkkainen MJ, Alitalo K, and Stacker SA, et al (2001). The specificity of receptor binding by vascular endothelial growth factor-d is different in mouse and man. *J Biol Chem* **276**, 19166–19171.

[20] Mandriota SJ, Jussila L, Jeltsch M, Compagni A, Baetens D, Prevo R, Banerji S, Huarte J, Montesano R, and Jackson DG, et al (2001). Vascular endothelial growth factor-C-mediated lymphangiogenesis promotes tumour metastasis. *EMBO J* **20**, 672–682.

[21] Skobe M, Hawighorst T, Jackson DG, Prevo R, Janes L, Velasco P, Riccardi L, Alitalo K, Claffey K, and Detmar M (2001). Induction of tumor lymphangiogenesis by VEGF-C promotes breast cancer metastasis. *Nat Med* **7**, 192–198.

[22] Stacker SA, Caesar C, Baldwin ME, Thornton GE, Williams RA, Prevo R, Jackson DG, Nishikawa S, Kubo H, and Achen MG (2001). VEGF-D promotes the metastatic spread of tumor cells via the lymphatics. *Nat Med* **7**, 186–191.

[23] Kopfstein L, Veikkola T, Djonov VG, Baeriswyl V, Schomber T, Strittmatter K, Stacker SA, Achen MG, Alitalo K, and Christofori G (2007). Distinct roles of vascular endothelial growth factor-D in lymphangiogenesis and metastasis. *Am J Pathol* **170**, 1348–1361.

[24] Harris NC, Paavonen K, Davydova N, Roufail S, Sato T, Zhang YF, Karnezis T, Stacker SA, and Achen MG (2011). Proteolytic processing of vascular endothelial growth factor-D is essential for its capacity to promote the growth and spread of cancer. *FASEB J* **25**, 2615–2625. http://dx.doi.org/10.1096/fj.10-179788.

[25] He Y, Kozaki K, Karpanen T, Koshikawa K, Ylä-Herttuala S, Takahashi T, and Alitalo K (2002). Suppression of tumor lymphangiogenesis and lymph node metastasis by blocking vascular endothelial growth factor receptor 3 signaling. *J Natl Cancer Inst* **94**, 819–825.

[26] Stacker SA, Williams RA, and Achen MG (2004). Lymphangiogenic growth factors as markers of tumor metastasis. *APMIS* **112**, 539–549.

[27] Achen MG, McColl BK, and Stacker SA (2005). Focus on lymphangiogenesis in tumor metastasis. *Cancer Cell* **7**, 121–127.

[28] Haiko P, Mäkinen T, Keskitalo S, Taipale J, Kärkkainen MJ, Baldwin ME, Stacker SA, Achen MG, and Alitalo K (2008). Deletion of vascular endothelial growth factor C (VEGF-C) and VEGF-D is not equivalent to VEGF receptor 3 deletion in mouse embryos. *Mol Cell Biol* **28**, 4843–4850. http://dx.doi.org/10.1128/MCB.02214-07.

[29] Abel EL, Angel JM, Kiguchi K, and DiGiovanni J (2009). Multi-stage chemical carcinogenesis in mouse skin: fundamentals and applications. *Nat Protoc* **4**, 1350–1362. http://dx.doi.org/10.1038/nprot.2009.120.

[30] Brideau G, Mäkinen MJ, Elamaa H, Tu H, Nilsson G, Alitalo K, Pihlajaniemi T, and Heljasvaara R (2007). Endostatin overexpression inhibits lymphangiogenesis and lymph node metastasis in mice. *Cancer Res* **67**, 11528–11535.

[31] Leder LD (1979). The chloroacetate esterase reaction. A useful means of histological diagnosis of hematological disorders from paraffin sections of skin. *Am J Dermatopathol* **1**, 39–42.

[32] Garaczi E, Széll M, Jánossy T, Koreck A, Pivarcsi A, Buzás E, Pos Z, Falus A, Dobozy A, and Kemény L (2004). Negative regulatory effect of histamine in DNFB-induced contact hypersensitivity. *Int Immunol* **16**, 1781–1788.

[33] Kar Mahapatra S, Bhattacharjee S, Chakraborty SP, Majumdar S, and Roy S (2011). Alteration of immune functions and Th1/Th2 cytokine balance in nicotine-induced murine macrophages: immunomodulatory role of eugenol and N-acetylcysteine. *Int Immunopharmacol* **11**, 485–495. http://dx.doi.org/10.1016/j.intimp.2010.12.020.

[34] Stober CB, Lange UG, Roberts MT, Alcami A, and Blackwell JM (2005). IL-10 from regulatory T cells determines vaccine efficacy in murine Leishmania major infection. *J Immunol* **175**, 2517–2524.

[35] Udalov S, Dumitrascu R, Pullamsetti S, Al-tamari HM, Weissmann N, Ghofrani HA, Guenther A, Voswinckel R, Seeger W, and Grimminger F, et al (2010). Effects of phosphodiesterase 4 inhibition on bleomycin-induced pulmonary fibrosis in mice. *BMC Pulm Med* **10**, 26. http://dx.doi.org/10.1186/1471-2466-10-26.

[36] Yang XO, Chang SH, Park H, Nurieva R, Shah B, Acero L, Wang Y-H, Schluns KS, Broaddus RR, and Zhu Z, et al (2008). Regulation of inflammatory responses by IL-17 F. *J Exp Med* **205**, 1063–1075. http://dx.doi.org/10.1084/jem.20071978.

[37] Smith E, Stark MA, Zarbock A, Burcin TL, Bruce AC, Vaswani D, Foley P, and Ley K (2008). IL-17A inhibits the expansion of IL-17A-producing T cells in mice through "short-loop" inhibition via IL-17 receptor. *J Immunol* **181**, 1357–1364.

[38] Kapil P, Atkinson R, Ramakrishna C, Cua DJ, Bergmann CC, and Stohlman SA (2009). Interleukin-12 (IL-12), but not IL-23, deficiency ameliorates viral encephalitis without affecting viral control. *J Virol* **83**, 5978–5986. http://dx.doi.org/10.1128/JVI.00315-09.

[39] Livak KJ and Schmittgen TD (2001). Analysis of relative gene expression data using real-time quantitative PCR and the 2(−Delta Delta C(T)) method. *Methods* **25**, 402–408.

[40] Sica A, Larghi P, Mancino A, Rubino L, Porta C, Totaro MG, Rimoldi M, Biswas SK, Allavena P, and Mantovani A (2008). Macrophage polarization in tumour progression. *Semin Cancer Biol* **18**, 349–355. http://dx.doi.org/10.1016/j.semcancer.2008.03.004.

[41] Zhu J, Yamane H, and Paul WE (2010). Differentiation of effector CD4 T cell populations. *Annu Rev Immunol* **28**, 445–489. http://dx.doi.org/10.1146/annurev-immunol-030409-101212.

[42] Bailey SR, Nelson MH, Himes R, Li Z, Mehrotra S, and Paulos CM (2014). Th17 cells in cancer: the ultimate identity crisis. *Front Immunol* **5**, 276. http://dx.doi.org/10.3389/fimmu.2014.00276.

[43] Alitalo AK, Proulx ST, Karaman S, Karaman S, Aebischer D, Martino S, Jost M, Schneider N, Bry M, and Detmar M (2013). VEGF-C and VEGF-D Blockade Inhibits Inflammatory Skin Carcinogenesis. *Cancer Res* **73**, 4212–4221. http://dx.doi.org/10.1158/0008-5472.CAN-12-4539.

[44] Yusuf N, Nasti TH, Katiyar SK, Jacobs MK, Seibert MD, Ginsburg AC, Timares L, Xu H, and Elmets CA (2008). Antagonistic roles of $CD4^+$ and $CD8^+$ T-cells in 7,12-dimethylbenz[a]anthracene cutaneous carcinogenesis. *Cancer Res* **68**, 3924–3930. http://dx.doi.org/10.1158/0008-5472.CAN-07-3059.

[45] Daniel D, Meyer-Morse N, Bergsland EK, Dehne K, Coussens LM, and Hanahan D (2003). Immune enhancement of skin carcinogenesis by $CD4^+$ T cells. *J Exp Med* **197**, 1017–1028.

[46] Zancope E, Costa NL, Junqueira-Kipnis AP, Valadares MC, Silva TA, Leles CR, Mendonça EF, and Batista AC (2010). Differential infiltration of CD8+ and NK cells in lip and oral cavity squamous cell carcinoma. *J Oral Pathol Med* **39**, 162–167. http://dx.doi.org/10.1111/j.1600-0714.2009.00792.x.

[47] Pettersen JS, Fuentes-Duculan J, Suárez-Fariñas M, Pierson KC, Pitts-Kiefer A, Fan L, Belkin DA, Wang CQ, Bhuvanendran S, and Johnson-Huang LM, et al (2011). Lowes MA, Carucci JA. Tumor-associated macrophages in the cutaneous SCC microenvironment are heterogeneously activated. *J Invest Dermatol* **131**, 1322–1330. http://dx.doi.org/10.103/jid.2011.9.

[48] Gabrilovich DI, Ostrand-Rosenberg S, and Bronte V (2012). Coordinated regulation of myeloid cells by tumours. *Nat Rev Immunol* **12**, 253–268. http://dx.doi.org/10.1038/nri3175.

[49] Wang H-W and Joyce JA (2010). Alternative activation of tumor-associated macrophages by IL-4. *Cell Cycle* **9**, 4824–4835.

[50] Udagawa T, Narumi K, Suzuki K, Aida K, Miyakawa R, Ikarashi Y, Makimoto A, Chikaraishi T, Yoshida T, and Aoki K (2013). Vascular endothelial growth factor-D-mediated blockade of regulatory T cells within tumors is induced by hematopoietic stem cell transplantation. *J Immunol* **191**, 3440–3452. http://dx.doi.org/10.4049/jimmunol.1201454.

[51] Huggenberger R, Ullmann S, Proulx ST, Pytowski B, Alitalo K, and Detmar M (2010). Stimulation of lymphangiogenesis via VEGFR-3 inhibits chronic skin inflammation. *J Exp Med* **207**, 2255–2269. http://dx.doi.org/10.1084/jem.20100559.

[52] Rinderknecht M and Detmar M (2008). Tumor lymphangiogenesis and melanoma metastasis. *J Cell Physiol* **216**, 347–354. http://dx.doi.org/10.1002/jcp.21494.

[53] Chauhan SK, Jin Y, Goyal S, Lee HS, Fuchsluger TA, Lee HK, and Dana R (2011). A novel pro-lymphangiogenic function for Th17/IL-17. *Blood* **118**, 4630–4634. http://dx.doi.org/10.1182/blood-2011-01-332049.

[54] Kozlowski M, Kowalczuk O, Milewski R, Chyczewski L, Niklinski J, and Laudanski J (2010). Serum vascular endothelial growth factors C and D in patients with oesophageal cancer. *Eur J Cardiothorac Surg* **38**, 260–267. http://dx.doi.org/10.1016/j.ejcts.2010.01.061.

[55] Sotiropoulou N, Bravou V, Kounelis S, Damaskou V, Papaspirou E, and Papadaki H (2010). Tumour expression of lymphangiogenic growth factors but not lymphatic vessel density is implicated in human cervical cancer progression. *Pathology* **42**, 629–636. http://dx.doi.org/10.3109/00313025.2010.522174.

[56] Szajewski M, Kruszewski WJ, Lakomy J, Ciesielski M, Kawecki K, Jankun J, Buczek T, and Szefel J (2014). VEGF-C and VEGF-D overexpression is more common in left-sided and well-differentiated colon adenocarcinoma. *Oncol Rep* **31**, 125–130. http://dx.doi.org/10.3892/or.2013.2821.